PCCP

The behavior of the iron(III)-catalyzed oxidation of ethanol by hydrogen peroxide in a fed-batch reactor

K.-P. Zeyer,*[a] S. Pushpavanam,[b] M. Mangold[a] and E. D. Gilles[a]

[a] *Max-Planck-Institut für Dynamik komplexer technischer Systeme, Leipziger Straße 44, 39120 Magdeburg, Germany*
[b] *Department of Chemical Engineering, Indian Institute of Technology Madras, Chennai (Madras) -600 036, India*

We present a theoretical (numerical) investigation of the exothermic iron(III) nitrate-catalyzed oxidation of ethanol with hydrogen peroxide to give ethanal and acetic acid. This reaction can display temperature and concentration oscillations when it is carried out in a continuous flow stirred tank reactor (CSTR) for some operating conditions. In this study we investigate the reaction when it is performed in a fed-batch reactor (FBR). The FBR can be interpreted as a mode of operation in between a CSTR and a batch reactor. The behavior of the reaction system is studied using two models. These differ in the degree of detail in evaluating properties. They hence have different degrees of complexity. The fed-batch mode of reactor operation is found to result in a significant improvement of the yield of ethanal, which is an intermediate product, in comparison to the batch and the CSTR modes of operation. The FBR mode of operation also introduces a rich variety of complex periodic states and chaos.

1 Introduction

Nonlinear thermokinetic reaction systems in a continuous flow stirred tank reactor (CSTR) can show a rich variety of complex dynamical states. The behavior of a first order thermokinetic reaction has been investigated in many studies.[1-5] This is described by one mass balance and one energy balance equation. The state space is therefore two-dimensional and complex behavior, such as bistability and period-1 oscillations, can be found. The system dynamics can become even more complex, exhibiting oscillatory states of higher periodicities or deterministic chaos, when the reaction schemes are more complex or when an additional degree of freedom is introduced, for example, by external forcing. For instance, a series reaction which consists of two exothermic first order reaction steps can display oscillations of higher periodicities and deterministic chaos.[6] Application of an external forcing, for example a periodic variation in the feed flow or the temperature, can also induce complex dynamic behavior in the system. In the continuously forced operation of a first order thermokinetic reaction, for example, Mankin and Hudson[7] found a period-doubling cascade to chaos. In addition, continuous external forcing was shown to give better yields, selectivities, or production rates of certain species in many studies of thermokinetic[8-10] as well as isothermal[11-12] systems.

A discrete way of externally forced operation of a reactor is the fed-batch operation mode (FBR). Here a fixed fraction of the reactor contents is discharged and replaced by fresh feed solution periodically at equally spaced time intervals. Codell and Engel[13] studied the isothermal and adiabatic operation of a controlled cycled tank reactor, which is identical to the FBR, and found advantages over a CSTR and a plug flow reactor. Ausikaitis and Engel[14] studied the reaction between sodium thiosulfate and hydrogen peroxide experimentally in such a reactor. Kubíčková *et al.*[15] and Konnur and Pushpavanam[16] investigated the nonlinear dynamics of a fed-batch operation mode of a first order exothermic reaction.

Period-doubling and period-adding cascades to chaos, quasi-periodicity, and mixed-mode oscillations were found.

In the present work we discuss the behavior of the FBR sustaining the ethanol oxidation reaction. Our objective is to determine if the yield of the intermediate ethanal can be improved in this mode of operation compared to the batch and the CSTR limits of operation. We also investigate the complex dynamic behavior induced by the discrete forcing. For this process, two models of different complexity are investigated. The nonlinear dynamic behavior of the two models is compared. We discuss and analyze the sensitivity of the behavior of the nonlinear system to the details included in the complex model.

2 Model system

2.1 Reaction scheme

Hafke and Gilles[17,18] demonstrated experimentally that the iron(III)-catalyzed oxidation of ethanol with hydrogen peroxide to give ethanal and acetic acid can display temperature and concentration oscillations in a CSTR. They derived a kinetic model based on elementary steps by applying the quasi-stationary state assumption to the intermediate species. The following reaction scheme was proposed by Hafke and Gilles:[17,18]
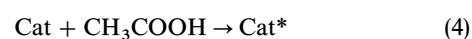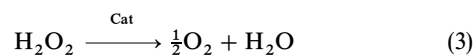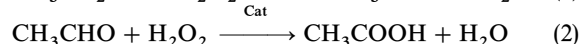
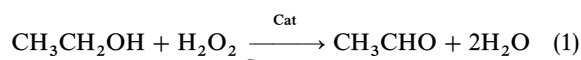$$CH_3CH_2OH + H_2O_2 \xrightarrow{\text{Cat}} CH_3CHO + 2H_2O \quad (1)$$

$$CH_3CHO + H_2O_2 \xrightarrow{\text{Cat}} CH_3COOH + H_2O \quad (2)$$

$$H_2O_2 \xrightarrow{\text{Cat}} \tfrac{1}{2}O_2 + H_2O \quad (3)$$

$$Cat + CH_3COOH \rightarrow Cat^* \quad (4)$$

$$Cat^* \rightarrow Cat + CH_3COOH \quad (5)$$

Table 1 Reaction enthalpies at $T = 298$ K and $p = 101\,325.0$ Pa used for the simple and the detailed model

	$-\Delta h_{\mathrm{R}}$/kJ mol^{-1}	
i	Simple model	Detailed model
1	302.0	302.5
2	389.0	385.9
3	95.0	95.1
4	0.0	0.0
5	0.0	0.0

Cat* denotes a catalytically inert acetato–iron(III) complex.[19] The reaction enthalpies ($-\Delta h_{\mathrm{R}}$) under standard conditions ($T = 298.15$ K and $p = 101\,325.0$ Pa) are given in Table 1. The dependence of the reaction rate constants on the temperature is described by the Arrhenius equation:[18]

The rate expressions we use read:[18]

$$r_1 = k_1\,e^{-E_1/RT}c_{\mathrm{Cat}}c_{\mathrm{H_2O_2}} \tag{6}$$

$$r_2 = k_2\,e^{-E_2/RT}c_{\mathrm{Cat}}c_{\mathrm{H_2O_2}}c_{\mathrm{CH_3CHO}} \tag{7}$$

$$r_3 = k_3\,e^{-E_3/RT}c_{\mathrm{Cat}}c_{\mathrm{H_2O_2}} \tag{8}$$

$$r_4 = k_4\,e^{-E_4/RT}c_{\mathrm{Cat}}\sqrt{c_{\mathrm{CH_3COOH}}} \tag{9}$$

$$r_5 = k_5\,e^{-E_5/RT}c_{\mathrm{Cat*}} \tag{10}$$

The preexponential factors k_i and energies of activation E_i are summarized in Table 2. Note that the reaction rate r_1 is independent of the ethanol concentration because ethanol is assumed to be in stoichiometric excess.[18]

2.2 Balance equations

The mass balances for the different species in a CSTR are:

$$\frac{dn_{\mathrm{H_2O}}}{dt} = \dot{q}_{\mathrm{f}}(c_{\mathrm{H_2O,f}} - c_{\mathrm{H_2O}}) + V_{\mathrm{L}}(2r_1 + r_2 + r_3) \tag{11}$$

$$\frac{dn_{\mathrm{H_2O_2}}}{dt} = \dot{q}_{\mathrm{f}}(c_{\mathrm{H_2O_2,f}} - c_{\mathrm{H_2O_2}}) - V_{\mathrm{L}}(r_1 + r_2 + r_3) \tag{12}$$

$$\frac{dn_{\mathrm{CH_3CH_2OH}}}{dt} = \dot{q}_{\mathrm{f}}(c_{\mathrm{CH_3CH_2OH,f}} - c_{\mathrm{CH_3CH_2OH}}) - V_{\mathrm{L}}(r_1) \tag{13}$$

$$\frac{dn_{\mathrm{CH_3CHO}}}{dt} = \dot{q}_{\mathrm{f}}(-c_{\mathrm{CH_3CHO}}) + V_{\mathrm{L}}(r_1 - r_2) \tag{14}$$

$$\frac{dn_{\mathrm{CH_3COOH}}}{dt} = \dot{q}_{\mathrm{f}}(-c_{\mathrm{CH_3COOH}}) + V_{\mathrm{L}}(r_2 - r_4 + r_5) \tag{15}$$

$$\frac{dn_{\mathrm{Cat}}}{dt} = \dot{q}_{\mathrm{f}}(c_{\mathrm{Cat,f}} - c_{\mathrm{Cat}}) - V_{\mathrm{L}}(r_4 - r_5) \tag{16}$$

$$\frac{dn_{\mathrm{Cat*}}}{dt} = \dot{q}_{\mathrm{f}}(-c_{\mathrm{Cat*}}) + V_{\mathrm{L}}(r_4 - r_5) \tag{17}$$

Here $\dot{q}_{\mathrm{f}}$ denotes the volumetric feed flow, n_i denotes the number of moles of species i in the reactor, $c_{i,\mathrm{f}}$ signifies the feed concentrations, and V_{L} is the volume of the liquid phase. The mass balance equation for ethanol is required to verify

Table 2 Preexponential factors k_i and energies of activation E_i used for both models

i	k_i	E_i/kJ mol^{-1}	Ref.
1	$1.494\,80 \times 10^{16}$ L mol^{-1} s^{-1}	105.50	18
2	$1.951\,32 \times 10^{20}$ L^2 mol^{-2} s^{-1}	126.20	18
3	$6.666\,00 \times 10^{14}$ L mol^{-1} s^{-1}	105.00	28
4	$1.176\,37 \times 10^{7}$ L$^{0.5}$ mol$^{-0.5}$ s^{-1}	55.69	18
5	$3.833\,30 \times 10^{4}$ s^{-1}	45.04	18

the assumption of ethanol being in excess. It is also necessary since the amount of ethanol influences the physical properties of the reaction mixture in the detailed model.

The energy balance for the system reads:

$$(\Gamma + \Gamma_{\mathrm{ins}})\frac{dT}{dt} = V_{\mathrm{L}}\sum_{i=1}^{3} r_i(-\Delta h_{\mathrm{R}})_i + P_{\mathrm{heat}}$$
$$+ P_{\mathrm{stirr}} - \dot{q}_{\mathrm{f}}(\rho c_{\mathrm{p}})_{\mathrm{f}}(T - T_{\mathrm{f}})$$
$$- (UA)_{\mathrm{loss}}(T - T_{\mathrm{amb}})$$
$$- (UA)_{\mathrm{cool}}(T - T_{\mathrm{cool,in}}) \tag{18}$$

Γ and Γ_{ins} are the total heat capacities of the liquid phase and the inserts, respectively. P_{heat} is the power introduced by the heating elements and P_{stirr} describes the power dissipated by the stirrer. T_{amb} is the ambient temperature. $(UA)_{\mathrm{loss}}$ signifies the overall heat transfer coefficient to the ambient. ρ_{f} and $c_{\mathrm{p,f}}$ denote the density and the specific heat capacity of the feed, respectively. T, T_{f} and $T_{\mathrm{cool,in}}$ are the reactor temperature, the temperature of the feed, and the temperature of the cooling water at the inlet of the cooling coil. $(UA)_{\mathrm{cool}}$ signifies the overall heat transfer coefficient, which describes the energy transfer from the reaction mixture to the coil.

2.3 The simple model

In the simple model all physical properties are assumed to be constant and independent of the actual composition of the reaction mixture. We assume the density ρ and the specific heat capacity c_{p} of the reactor contents to be that of water, which forms 78 wt.% of the feed. This yields $\rho = 1.0$ kg L^{-1} and $(\rho c_{\mathrm{p}})_{\mathrm{f}} = 4200.0$ kJ m^{-3} K^{-1} for the feed as well as for the reactor contents. The thermal capacity of the inserts Γ_{ins} is taken as 2290 J K^{-1} and that of the reactor contents Γ is 10080 J K^{-1} according to a reaction volume V_{L} of 2.4 L of water. The power supplied by the heating element P_{heat} is taken as 1600 W. The temperature dependence of the reaction enthalpies $-\Delta h_{\mathrm{R}}$ is neglected and the values given for standard conditions are always used (see Table 1). In the simple model the power dissipated by the stirrer P_{stirr} and the heat transfer to the ambient $-(UA)_{\mathrm{loss}}(T - T_{\mathrm{amb}})$ are neglected in the energy balance equation [eqn. (18)] by setting P_{stirr} and $(UA)_{\mathrm{loss}}$ to 0.

The heat transfer coefficient from the reaction mixture to the coolant $(UA)_{\mathrm{cool}}$ is used directly as a bifurcation parameter. The feed concentrations (weight fractions) of water, hydrogen peroxide, ethanol, and catalyst are taken as 43.33 mol L^{-1} ($w_{\mathrm{H_2O,f}} = 0.78$), 2.94 mol L^{-1} ($w_{\mathrm{H_2O_2,f}} = 0.10$), 2.17 mol L^{-1} ($w_{\mathrm{CH_3CH_2OH,f}} = 0.10$) and 0.05 mol L^{-1} ($w_{\mathrm{Cat,f}} = 0.02$), respectively. The feed temperature is taken as 288 K and the coolant temperature is assumed to be 278 K. The volumetric flow rate of the feed $\dot{q}_{\mathrm{f}}$ is assumed to be 5.93 L h^{-1} so that it results in a hydrodynamic residence time or space time τ of 1457 s. The space time here is defined as:

$$\tau = \frac{m_{\mathrm{L}}}{\dot{q}_{\mathrm{f}}\rho_{\mathrm{f}}} \tag{19}$$

where m_{L} is the mass of the liquid phase. For a CSTR with no density changes the space time is the same as the residence time. We use the space time instead of the residence time because we keep the mass of the reactor contents constant in the detailed model instead of the volume.

2.4 The detailed model

The temperature dependence of the reaction enthalpies as well as that of other physical properties, such as the densities or the heat capacities, is evaluated in the detailed model using correlations given in the DIPPR catalogue.[20] The dynamics of

the wall of the cooling coil and the coolant are assumed to be in the quasi-steady state for the operating conditions. The heat transfer coefficients on the mixture and the coolant side are calculated based on correlations from the *VDI-Wärmeatlas*.[21] These correlations have been optimized with a parameter identification of dynamic experiments[22] at different stirrer speeds, coolant flows, and heating powers. The values of the heat capacity Γ_{ins} of the inserts and the overall heat transfer coefficient $(UA)_{loss}$ to the ambient that we use in the simulations are 2290 J K^{-1} and 6.6 W K^{-1}, respectively.[23]

In the detailed model the volumetric coolant flow rate $\dot{q}_{cool}$ is used directly as the bifurcation parameter instead of the previously used heat transfer coefficient $(UA)_{cool}$. The heat transfer coefficient $(UA)_{cool}$ is calculated from the coolant flow rate $\dot{q}_{cool}$. In the Appendix the calculation of the heat transfer to the cooling coil is described in detail and the relation between $(UA)_{cool}$ and the volumetric coolant flow rate $\dot{q}_{cool}$ is given.

The reaction mass m_L is maintained constant at $m_L = 2455.0$ g, which corresponds to a volume of $V_L = 2.4$ L using the conditions given in the caption of Fig. 2(a) and a coolant flow rate $\dot{q}_{cool} = 140.3$ L h^{-1}. In the detailed model the liquid volume V_L is evaluated from the physical properties of all the components. V_L varies during the course of the reaction, whereas the mass of the liquid phase m_L is kept constant at 2455.0 g *via* a p-controller for the outlet pump. The volumetric flow rate of the feed $\dot{q}_f$ is set to 5.93 L h^{-1} and the density of the feed ρ_f is 1.036 kg L^{-1} for the feed composition used [see the caption of Fig. 2(a)]. These values give a space time of $\tau = 1438$ s.

This kinetic model describes the steady state behavior of the CSTR and its stability characteristics accurately. It can also be used to determine the operating conditions under which the CSTR exhibits limit cycle behavior. Numerical and experimental results for different parameter sets are reported in refs. 24 and 25.

3 Dynamics of the models in a CSTR

The models are analyzed numerically by integration and continuation of steady states and periodic solutions using the simulation package DIVA.[26] It is also possible to determine the stability of stationary solutions and limit cycles *via* calculation of the eigenvalues of the Jacobi matrix and the Floquet multipliers, respectively, using this package.

3.1 The simple model

In this section we discuss the behavior of the simple model. The CSTR and the batch modes of operation are considered here. The performance of the CSTR is studied as a function of the bifurcation parameter $(UA)_{cool}$, the heat transfer coefficient to the cooling coil. This is a convenient choice for a bifurcation parameter as it can be varied experimentally by changing the coolant flow rate. The reaction scheme [eqns. (1)–(5)] can be visualized as a series reaction network with ethanal being an intermediate product. The production of the intermediate product can be maximized at some optimum operating conditions. Thus, for a fixed set of all other parameters, the concentration of the intermediate ethanal in the CSTR exhibits a maximum for a given space time τ. For space times lower than this the rate of formation of the intermediate is very low. For space times larger than this the intermediate product ethanal formed reacts and gives rise to acetic acid. This optimum in the product concentration as a function of a parameter also exists with respect to the bifurcation parameter $(UA)_{cool}$ for a fixed space time τ. This is depicted in Fig. 1 where we have plotted the ratio of the exit concentration of ethanal to the feed concentration of ethanol *vs.* the bifurcation parameter $(UA)_{cool}$. The ordinate is a measure of the yield and
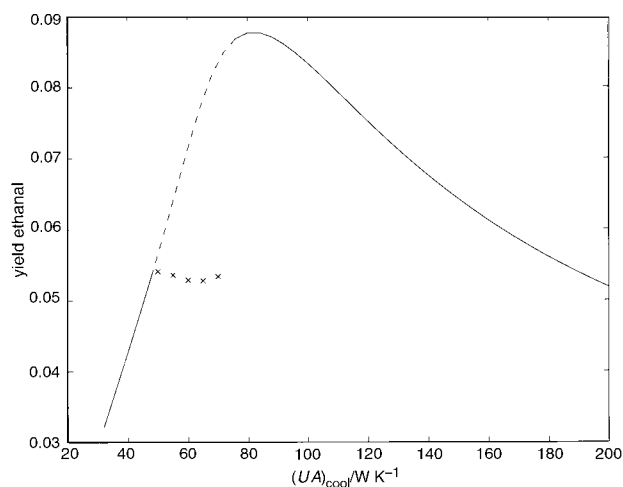

Fig. 1 Simple model. Bifurcation diagram showing ethanal yield (average concentration of ethanal in the reactor divided by feed concentration of ethanol) *vs.* heat transfer coefficient $(UA)_{cool}$. The solid line signifies regions of stable steady states, whereas the dashed line signifies unstable steady states; crosses mark the average ethanal yields corresponding to stable limit cycle oscillations. Parameters: weight fractions in feed, $w_{H_2O_2, f} = 0.10$, $w_{CH_3CH_2OH, f} = 0.10$, $w_{Cat, f} = 0.02$. Other conditions: $T_f = 15.0\,°C$, $T_{cool, in} = 5.0\,°C$, $\dot{q}_f = 5.93$ L h^{-1}, $P_{heat} = 1600$ W.

represents the moles of intermediate formed per mole of ethanol fed. It attains a maximum of 0.088 when the bifurcation parameter $(UA)_{cool}$ is 82 W K^{-1}. The steady states are dynamically unstable when the bifurcation parameter $(UA)_{cool}$ lies between 49 and 76 W K^{-1}. A supercritical Hopf bifurcation occurs at $(UA)_{cool} = 49$ W K^{-1} and a subcritical Hopf bifurcation occurs at $(UA)_{cool} = 76$ W K^{-1}. Inside this interval the system shows limit cycle oscillations. The limit cycles have a large amplitude for $(UA)_{cool}$ values just below 76 W K^{-1}. For $(UA)_{cool}$ values greater than 49 W K^{-1} the limit cycle oscillations have a small amplitude, which increases as we increase $(UA)_{cool}$ beyond 49 W K^{-1}. This confirms the nature of the bifurcations. The performance of the batch reactor is simulated for the same operating conditions. The batch reaction time is chosen as the space time of the CSTR, *i.e.* 1457 s. The yield found at the end of the reaction time is 0.0066 when the $(UA)_{cool}$ parameter is chosen as 82 W K^{-1}. During the course of the batch reaction the yield of the intermediate increases to 0.082 at a reaction time of 355 s and then drops to 0.0066 at the end of the cycle. This is accompanied by a high temperature excursion in the batch mode of operation.

3.2 The detailed model

In this section we describe the behavior of the CSTR and batch modes of operation for the detailed model. Fig. 2(a) shows a bifurcation diagram obtained by continuation of stationary and periodic solutions using the detailed model. A region of periodic solutions is traversed when the coolant flow $\dot{q}_{cool}$ is increased. An important result is the existence of a supercritical and a subcritical Hopf bifurcation point at $\dot{q}_{cool} = 55.36$ L h^{-1} and $\dot{q}_{cool} = 111.07$ L h^{-1}, respectively. The periodic solutions near the supercritical Hopf point show small temperature amplitudes (soft generation of limit cycles). Therefore, passing this Hopf bifurcation is a safe way to enter the region of periodic solutions. In contrast, the transition from steady states at high coolant flow rates to the region of periodic solutions by passing the subcritical Hopf point will lead to a sudden onset of oscillations with high temperature peaks and is therefore hazardous (hard generation of limit cycles). At low coolant flows the conversion of ethanol and hydrogen peroxide is high and a high yield of acetic acid can
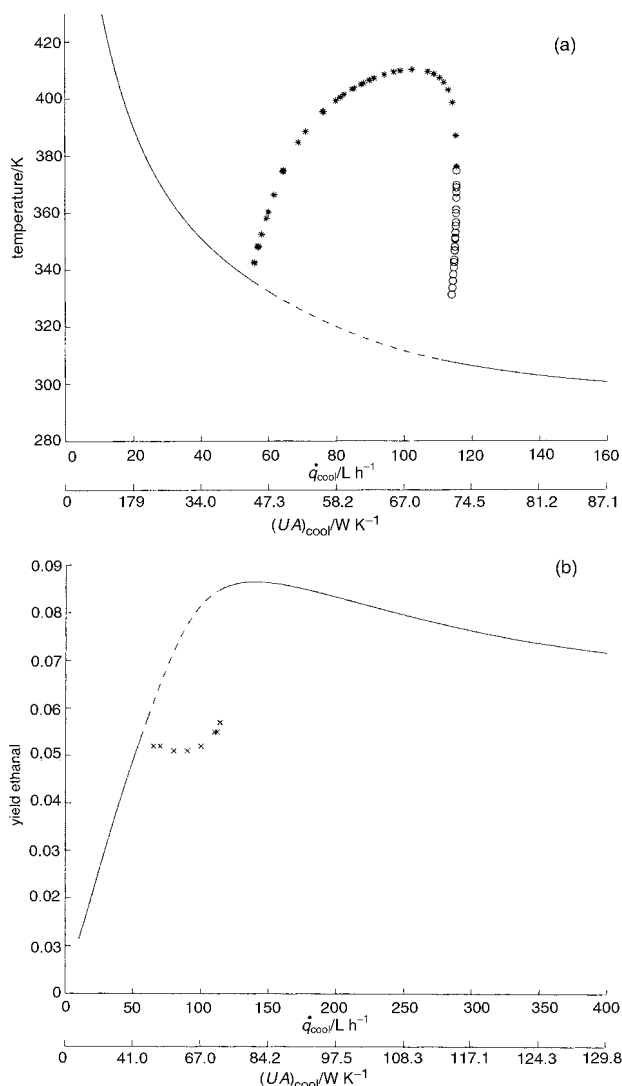
Fig. 2 Detailed model. (a) Bifurcation diagram showing the regions of stationary and periodic solutions. Stable and unstable steady states are indicated by solid and dashed lines, respectively; the asterisks and the open circles show the temperature maxima of the observed stable and unstable limit cycle oscillations, respectively. Parameters: weight fractions in the feed, $w_{H_2O_2, f} = 0.10$, $w_{CH_3CH_2OH, f} = 0.10$, $w_{Cat, f} = 0.02$. Other conditions: $T_f = 15.0\,°C$, $T_{cool, in} = 4.83\,°C$, $T_{amb} = 21.7\,°C$, number of rotations of the stirrer $N_{stirr} = 500\ min^{-1}$, $\dot{q}_f = 5.93\ L\ h^{-1}$, $P_{heat} = 1600\ W$. (b) The time average yield of ethanal plotted *vs.* the volumetric coolant flow $\dot{q}_{cool}$ and the heat transfer coefficient $(UA)_{cool}$. The solid and the dashed lines signify stable and unstable stationary solutions, respectively; crosses mark the time average yield corresponding to stable oscillatory states. Same parameter set as in part (a).

be achieved. In contrast, at high coolant flow rates both conversions are low so that high concentrations of hydrogen peroxide and ethanol accumulate in the reactor and react quickly away in a strongly exothermic reaction when the subcritical Hopf point is crossed, which is a potential source of danger. In Fig. 2(b) the yield of ethanal is given as a function of the coolant flow rate $\dot{q}_{cool}$. The yield of ethanal is very low at low coolant flows and passes through a maximum (0.0866) at $\dot{q}_{cool} = 140.3\ L\ h^{-1}$ near the subcritical Hopf point. The dynamically unstable range of CSTR operation for both models occurs in the portion of the bifurcation diagram where the yield of the intermediate increases with increasing heat transfer coefficient or coolant flow rate, *i.e.* left of the point of maximum yield [see Figs. 1 and 2(b)]. The time average of the ethanal yield in an oscillatory state is lower than the yield corresponding to the unstable steady state at the same value of the bifurcation parameter [Figs. 1 and 2(b)]. In Figs. 2(a) and (b) we represent both the $\dot{q}_{cool}$ and $(UA)_{cool}$ values along

the x-coordinate. This is to facilitate the comparison with Fig. 1.

4 Fed-batch operation mode

The volume (mass) of the reactor contents is initially V_0 (m_0). The repeated FBR mode of operation is characterized by the following steps (Fig. 3):

(i) A fixed mass Δm of fresh feed is added to maintain the mass in the reactor at m_L.

(ii) The reactor contents are well stirred and the reaction is allowed to occur in batch mode for P time units.

(iii) A mass Δm of the reactor contents containing unconverted reactants and products is discharged.

(iv) The cycle of steps (i)–(iii) is repeated.

The steps (i) and (iii) are assumed to be instantaneous in the simple model. This assumption is valid when their duration is small compared to the time of the batch reaction step (ii). We discuss the behavior of the FBR mode of operation for the parameter sets given in the captions of Figs. 1 and 2(a) for the simple model and the detailed model, respectively.

In the case of the FBR the space time τ is given by:

$$\tau = \frac{P}{R} \qquad (20)$$

with

$$R = \frac{\Delta m}{m_L}$$

where R is the ratio of mass Δm that is discharged and replaced by fresh feed to the total reaction mass in the reactor (m_L). P signifies the reaction time in the batch mode during which no reactants are fed or removed. For the discharge of product and addition of feed, time intervals of 1 s each are chosen for the detailed model. During these intervals the reaction proceeds. The FBR is investigated such that the space time P/R is always kept constant and equal to the space time of the CSTR. This ensures a fair comparison between the two modes of operation. For the limit

$$\lim_{R \to 0,\, P \to 0} \frac{P}{R} = \tau \quad \text{(finite)} \qquad (21)$$

the FBR approaches the operation of a CSTR, whereas for $R \to 1$ the FBR reaches a batch reactor which is charged every P seconds.

The evolution of the moles of species i during the batch operation is governed by eqns. (11)–(18) with $\dot{q}_f = 0$. The fresh feed addition and the removal of products for species i is assumed to be instantaneous in the simple model. The mass balance of species i at these time instants is:

$$c_i(P^+) = (1 - R)c_i(P^-) + Rc_{i, f}, \qquad (22)$$

where $R = \Delta m/m_L$ and $m_0/m_L = 1 - R$. The instantaneous removal and addition results in a discontinuity in the concen-
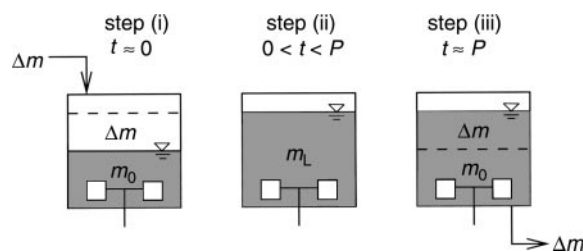

Fig. 3 Schematic description of the FBR mode. Step (i): Fresh feed of mass Δm is added to the reactor. The mass increases from m_0 to m_L. Step (ii): During the batch reaction time P inflow and outflow are switched off. Step (iii): The mass Δm is withdrawn from the reactor. The mass is reduced from m_L to m_0. The steps (i) (charging), (ii) (batch reaction) and (iii) (discharging) are repeated subsequently.

trations every P units. This is reflected in the updating conditions. Here P^- and P^+ denote the time instant before and after the instantaneous discharge and feed addition, and c_i and $c_{i,f}$ signify the concentration of species i in the reactor and in the feed, respectively. The FBR is governed by integrating the batch reactor equations for a cycle, *i.e.* P units. The initial conditions of the next cycle, *i.e.* at P^+, are determined by the updating conditions. This sequence of integration and updating is cyclically repeated. The basic state of the FBR operation is the periodic state with period P. This is called the period-1 (1P) solution and it is analogous to the steady state of the CSTR. The fed-batch operation is hence a periodically forced operation of a batch reactor with the forcing occurring at discrete points of time.

5 Results

5.1 The simple model

The operation of the repeated FBR is now discussed. In this mode of operation the space time τ is always chosen as equal to that of the CSTR. The fraction R, that is discharged and added is varied from 0.05 to 0.95. The batch reaction time P is varied simultaneously to maintain the space time of 1457 s. The concentration of ethanal at the end of the reaction period is representative of the production rate or yield since this is the composition that is withdrawn or harvested. The value of $(UA)_{cool}$ is again chosen as 82 W K^{-1} (where the maximum yield of the CSTR occurred). In the FBR mode of operation we have an added degree of freedom which helps us to maintain the space time. This is the parameter R which can be varied along with P to satisfy the constraint of having the same space time τ. The basic state in this mode of operation is the periodic state with period equal to the reaction period P. This is called the 1P solution. As we vary the parameter R, maintaining the space time constant at $\tau = 1457$ s, the system exhibits complex dynamic behavior. In particular we find period-2, period-3, period-4, period-5, and period-9 solutions in addition to the basic period-1 solution. In a period-m state the period of the solution is m times the forcing period. A summary of the behavior of this mode of operation is shown in Table 3. The system follows a basic period-adding sequence (period-1, period-2, …, period-5). Additional period-m solutions are located between a period-k solution and a period-l solution such that $m = l + k$. A 5P solution is generated by the interaction of a 1P solution and a 4P solution. Similarly a 9P solution arises by the interaction of a 5P solution and a 4P solution. The variation of the yield of ethanal with the parameter P is shown in Table 3 as well as in Fig. 4. We find that the yield increases from the CSTR value of 0.088 in the limit of R tending to zero to a maximum value of 0.1032 at $P = 654$ s. This is an improvement of around 15% over the optimal yield of the CSTR for the same set of operating conditions, *i.e.* feed and space time. Beyond this value of P, the 1P solution of the system is unstable. We see oscillations whose period is five times the batch reaction time, *i.e.* a 5P state at $P = 670$ s, a 4P state at $P = 772$ s, a 9P state at $P = 729$ s, a 7P state at $P = 780$ s, *etc.* From $P = 1020$ s to 1122 s dynamic simulations yield a 2P state. The yield obtained in these states, where the period is greater than P, is found by averaging over the concentrations that are withdrawn from the reactor. Thus, for the 2P state at $P = 1122$ s the yield harvested alternates between 0.0997 and 0.0089. This is accompanied by a large temperature oscillation and a small temperature oscillation in the two halves of the periodic state. The average yield for these operating conditions is 0.0543. As P approaches the space time τ the yield of the reactor approaches that of the batch operation, *i.e.* 0.0069. This is accompanied by oscillations which have only large temperature peaks. The small temperature peak oscillation disappears as P approaches τ.

We depict the yield of ethanal as a function of the parameter P in Fig. 4. There is an increase in the yield till P reaches a value of 654 s. Beyond this the yield drops. This is accompanied by the onset of high period oscillations as can be seen in Table 3. These high period oscillations are characterized by high temperature peaks. In the limit of the FBR mode of operation approaching the batch limit the low temperature half of the cycle disappears and the 1P solution which exists from $P = 1239$ s to $P = 1457$ s is characterized by low yield values and associated with the high temperature peaks of the cycle.

We also study the behavior the the FBR for $(UA)_{cool} = 35$ W K^{-1}. For this low value of the heat transfer coefficient parameter the CSTR shows a high temperature steady state. The yield of ethanal at this steady state is 0.0361 in the CSTR (Fig. 1). We investigate the FBR mode of operation for this parameter set and increase P gradually. First, the yield of ethanal increases slightly ($P = 73$ s, yield = 0.0385) above the corresponding yield obtained in the CSTR. Further increasing P the yield decreases ($P = 219$ s, yield = 0.0370; $P = 364$ s, yield = 0.0315; $P = 510$ s, yield = 0.0248) and approaches the

Table 3 Dynamical behavior of the simple model in the FBR; $(UA)_{cool} = 82$ W K^{-1}; other parameters are given in the caption of Fig. 1

P/s	Dynamical state response period/forcing period P	Ethanal yield
73	1P	0.090
219	1P	0.094
364	1P	0.097
510	1P	0.101
583	1P	0.102
627	1P	0.103
654	1P	0.103
659	5P	0.064
670	5P	0.058
685	5P	0.049
699	5P	0.050
729	9P	0.059
772	4P	0.045
780	7P	0.050
845	3P	0.059
918	5P	0.058
1020	2P	0.047
1093	2P	0.052
1122	2P	0.054
1239	1P	0.012
1311	1P	0.009
1384	1P	0.008

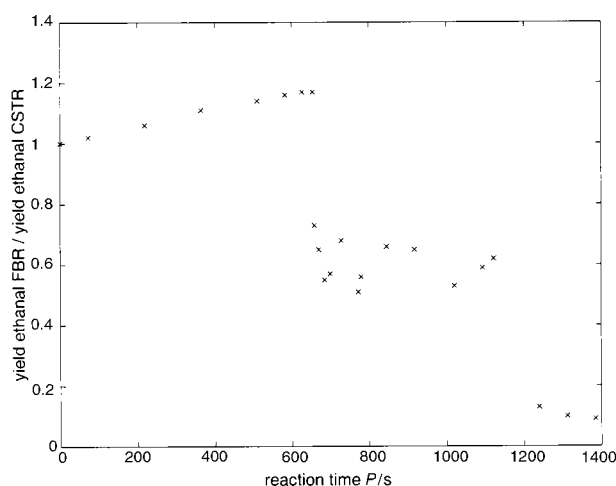**Fig. 4** Simple model. Fed-batch mode; same parameter set as in Fig. 1. $(UA)_{cool} = 82$ W K^{-1} (maximum yield of ethanal in the CSTR). The average yield of ethanal divided by the respective yield of ethanal in the CSTR (0.088) is depicted *vs.* the reaction time P.
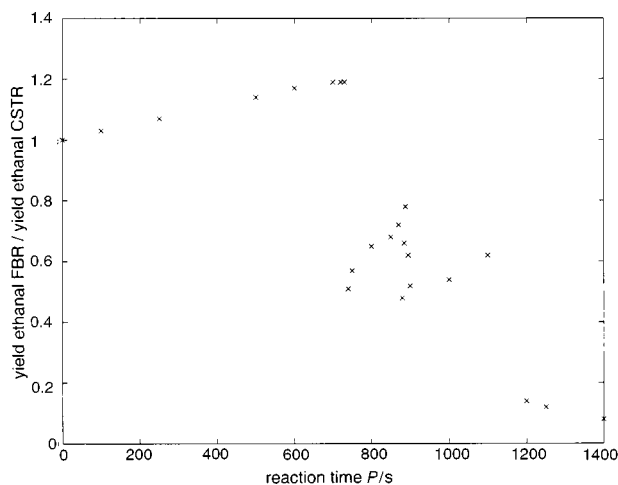
Fig. 5 Detailed model. Fed-batch mode; same parameter set as in Fig. 2(a). Volumetric flow rate of the coolant water $\dot{q}_{cool} = 140.3$ L h^{-1} (maximum yield of ethanal in the CSTR). The average yield of ethanal divided by the respective yield of ethanal in the CSTR (0.0866) *vs.* the reaction time P is shown.

yield of the batch reactor (0.0056) for $R \rightarrow 1$. The yield in the batch reactor attains a maximum of 0.068 at a reaction time of 180 s and then drops to the value of 0.0056 suddenly. For all the values of P simulated above only period-1 states are obtained.

Additionally, we study the behavior of the FBR for $(UA)_{cool} = 60$ W K^{-1}. For this operating condition the CSTR shows limit cycle oscillations. The yield of ethanal corresponding to the unstable steady state is found to be 0.0714, whereas an average yield of 0.0529 is found for ethanal on the stable limit cycle (Fig. 1). In the FBR mode for this value of the bifurcation parameter the yield drops down without increasing above the yield of the CSTR [$P = 73$ s, yield = 0.0544 (quasiperiodic); $P = 219$ s, yield = 0.0531 (quasiperiodic); $P = 291$ s, yield = 0.0464 (6P solution); $P = 364$ s, yield = 0.0474 (5P solution); $P = 510$ s, yield = 0.054 (3P solution); $P = 801$ s, yield = 0.04 (2P solution)]. The yields reported here are average values as discussed earlier. The variation of the yield with P is not monotonic. We find quasi-periodic responses for low values of P. This arises due to the

Table 4 Dynamical behavior of the detailed model in the FBR; $\dot{q}_{cool} = 140.3$ L h^{-1}; other parameters are given in the caption of Fig. 2(a)

P/s	Dynamical state Response period/forcing period P	Ethanal yield
100	1P	0.089
250	1P	0.093
500	1P	0.099
732	1P	0.103
733	4P	0.041
740	4P	0.044
750	7P	0.049
800	3P	0.056
850	3P	0.059
870	3P	0.062
880	C	0.042
881	8P	0.050
882	8P	0.049
883	5P	0.058
885	5P	0.057
888	7P	0.068
895	C	0.054
900	2P	0.045
1000	2P	0.047
1100	2P	0.054
1200	1P	0.012
1400	1P	0.007

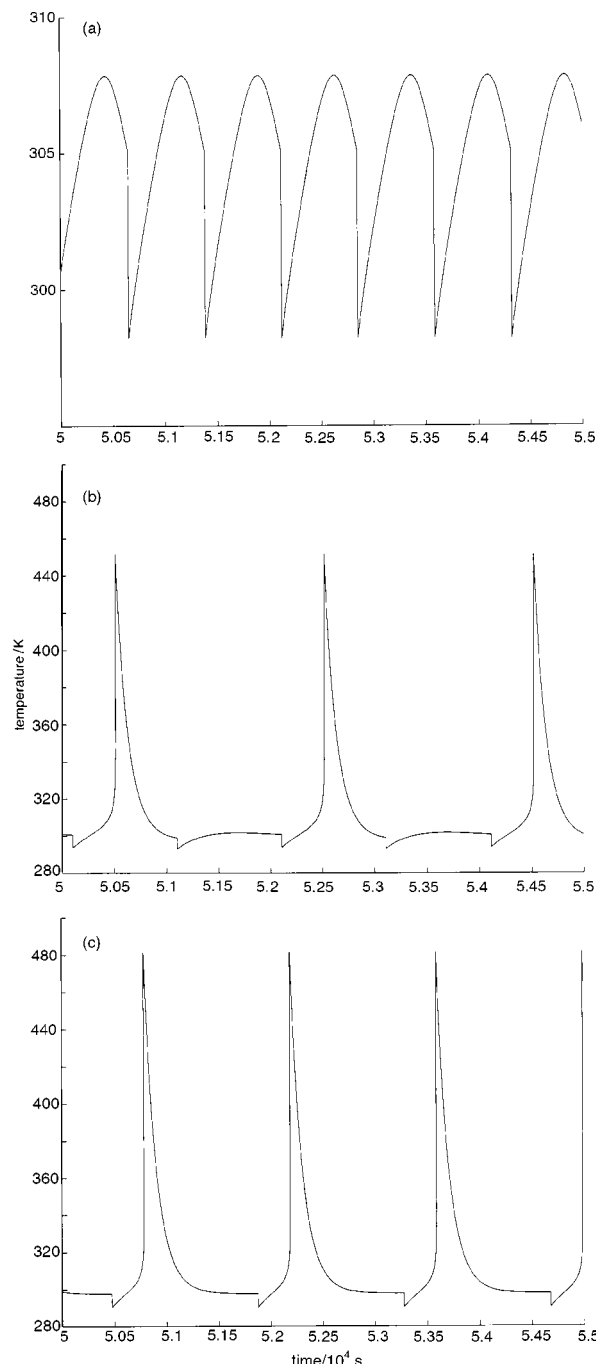**Fig. 6** Detailed model. Fed-batch mode; $\dot{q}_{cool} = 140.3$ L h^{-1}; other parameters are given in caption of Fig. 2(a); time series obtained for (a) $P = 732$ s (maximum ethanal yield), (b) $P = 1000$ s, (c) and $P = 1400$ s, respectively, showing small period-1 oscillations, period-2 oscillations, and large period-1 oscillations.

fact that in this case the time period of the autonomous oscillations of the CSTR in the limit of P tending to zero interacts with the forcing period P of the FBR. We find periodic behavior for high values of the parameter P. For this value of the heat transfer coefficient the batch reactor yield increases to a maximum of 0.073 in 240 s and then drops to 0.0059 at the time of 1457 s.

5.2 The detailed model

In the detailed model the reactor is assumed to be initially filled with 2455.0 g of an aqueous solution containing 23.0 wt.% ethanol and 1.9 wt.% catalyst. The volumetric coolant flow rate is fixed at $\dot{q}_{cool} = 140.3$ L h^{-1}, where the CSTR shows a maximum yield of ethanal [Fig. 2(b)]. All other parameters are the same as given in the caption of Fig. 2(a).

The FBR is modeled by switching on the outflow for 1 s so that the desired fraction R of the reaction mass m_L is removed. Then, the feed is switched on for 1 s to fill the reactor up to the original mass again. During the reaction phase for P units the outflow and the inflow are switched off. This is repeated cyclically. Fig. 5 shows the yield of ethanal obtained by the fed-batch operation *vs.* the reaction time P. At the left hand side of the diagram the yield of ethanal converges to the yield obtained in the CSTR (0.0866) [see Fig. 2(b)], because for $R \to 0$ and $P \to 0$ the FBR approaches the CSTR. For increasing reaction times P the yield of ethanal is increasing up to a maximum of 0.103 at $P = 732$ s. Further increasing P causes the yield to drop down below the value obtained for the CSTR. In this region some irregularities of the yield are found. A further decline occurs when P is increased above 1100 s. Finally, for $R = 1.0$ and $P = 1438.1$ s the batch limit is reached, because the whole reactor content is discharged and charged periodically. In the batch limit the yield of ethanal is 0.007.

Table 4 gives an overview of the observed dynamical states that evolve in the fed-batch operation mode. For the CSTR limit ($R \to 0$ and $P \to 0$) a steady state is reached. Since the fed-batch mode is a kind of forced operation, the simplest response dynamics must be a period-1 limit cycle.[16] Period-1 response is found for increasing P up to 732 s. In this region the yield improvement occurs as seen for the simple model. The significant decline of the yield above $P = 732$ s is accompanied by the occurrence of complex periodic oscillations, which consist of small and large temperature amplitudes. The second decline of the yield above $P = 1100$ s is connected with the transition of the mixed-mode oscillations to pure period-1 oscillations. In contrast to the period-1 oscillations observed between $P = 0$ and 732 s, these oscillations consist of high temperature oscillations. In practice and in the light of process safety these high temperature excursions can be interpreted as thermal runaways. For illustration Fig. 6(a)–(c) show time series obtained at $P = 732$ s, $P = 1000$ s and $P = 1400$ s, respectively, where the FBR shows small period-1 oscillations (maximum ethanal yield), period-2 responses and large period-1 oscillations near the batch limit.

Table 4 shows that, between the regions of small and large period-1 response amplitudes, a region of complex-periodic (mixed-mode) and chaotic oscillations emerges. Here a similar structure of dynamical states is found as in the simple model. We find a basic sequence of period-added states (1P, 2P, 3P, 4P; see Table 4). Between the states of this series we get periodicities which are composed by the addition of the periods of the individual neighbor states. We observe a 5P state between the 2P and the 3P state, and a 7P state between the 3P and the 4P state, for example. This principle continues further on by forming a 8P (3P and 5P neighbors) and a 7P (5P and 2P neighbors) state accordingly. We assume that there are many more states with high periods existing in this sequence, which emerge in very small intervals of P. An aperiodic time series obtained at $P = 895$ s is depicted in Fig. 7(a). Fig. 7(b) shows the corresponding stroboscopic map, which shows a complex structure typical for chaotic behavior. The stroboscopic map is constructed by plotting the temperature value at a given time $t + P + 2$ s *vs.* the temperature at time t. The value of 2 s is necessary to account for the charging and discharging time. In the stroboscopic map representation a period-n state shows n points. In addition, we determine the three largest Lyapunov exponents to be positive, zero and negative, respectively, which is further evidence for the deterministic chaotic origin of the observed aperiodicity.

As in the simple model we investigate the behavior of the FBR starting on a stationary state which is located on the high temperature branch of stationary states. Using the coolant flow rate $\dot{q}_{cool} = 30$ L h^{-1} we get a steady state at
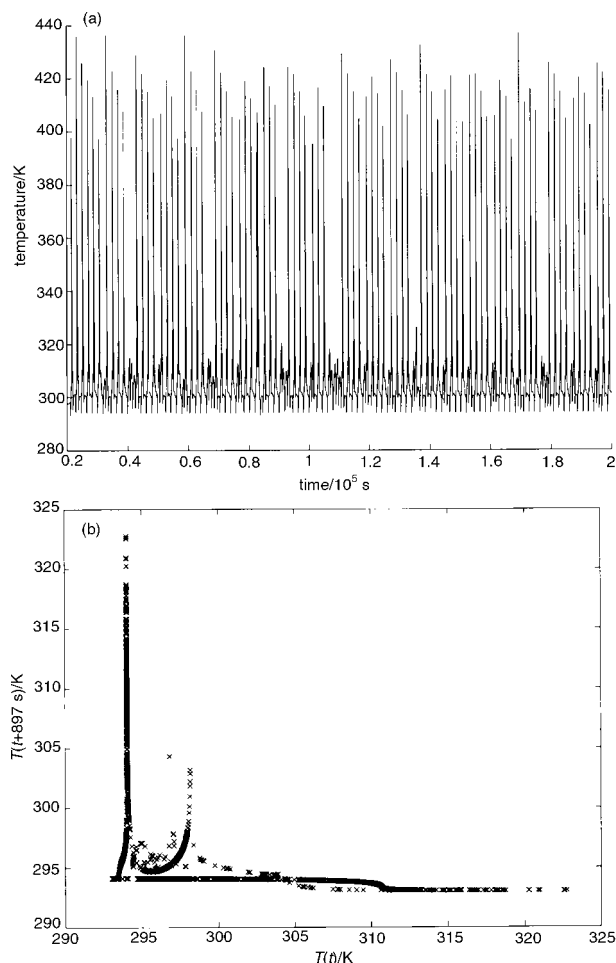

Fig. 7 Detailed model. Fed-batch mode; $\dot{q}_{cool} = 140.3$ L h^{-1}; other parameters are given in caption of Fig. 2(a); (a) time series obtained for $P = 895$ s showing chaotic behavior. (b) Stroboscopic map corresponding to the time series shown in part (a). The temperature at time $t + P + 2$ s ($P = 895$ s) is depicted *vs.* the temperature at time t.

366.3 K and an ethanal yield of 0.031 [Fig. 2(a) and (b)]. We investigate the FBR mode of operation by increasing P gradually. For low values of P the yield increases a little bit and then declines as in the simple model ($P = 50$ s, yield = 0.032; $P = 100$ s, yield = 0.032; $P = 200$ s, yield = 0.030; $P = 500$ s, yield = 0.020; $P = 1000$ s, yield = 0.010). Only period-1 responses are found as in the simple model.

Finally, we investigate the FBR behavior for a coolant flow rate where the CSTR shows dynamic instability. For $\dot{q}_{cool} = 100.0$ L h^{-1} we find period-1 oscillations. The corresponding average yield of ethanal is 0.052 for the oscillatory state and 0.082 for the unstable steady state, respectively [Fig. 2(b)]. When the FBR mode is applied and P is increased, the yield of ethanal increases slightly ($P = 100$ s, yield = 0.054; $P = 250$ s, yield = 0.054). Further increasing P the yield shows significant fluctuations until it finally drops down, approaching the yield of the batch reactor ($P = 300$ s, yield = 0.045; $P = 400$ s, yield = 0.037; $P = 450$ s, yield = 0.054; $P = 485$ s, yield = 0.044; $P = 500$ s, yield = 0.036; $P = 750$ s, yield = 0.042; $P = 1000$ s, yield = 0.015). The dynamics are very complex as in the simplified model. For low P values quasiperiodic states are found ($P = 200$ s, $P = 250$ s and $P = 450$ s, for example). Regions of high periodic states are observed in addition ($P = 100$ s, 22P; $P = 115$ s, 19P) where the forcing period and the response period of the system are entrained in a ratio of natural numbers. For increasing P values periodic states with decreasing periods exist ($P = 300$ s, 7P; $P = 350$ s, 6P; $P = 400$ s, 5P; $P = 500$ s, 4P; $P = 600$ s, 3P; $P = 900$ s, 2P) until 1P states emerge finally for $P > 940$ s.

6 Discussion

In this paper we analyze the behavior of a system of reactions in a CSTR and in the repeated fed-batch mode of operation. The reaction network can be thought of as a series reaction. The repeated fed-batch mode of operation is shown to result in a better yield than the optimal value attained in the CSTR. This occurs because an extra degree of freedom is available to maintain the same space time as that of the CSTR. The behavior of two different models is compared in this paper. In one the physical properties are treated as a constant, and in the other detailed correlations are used to estimate the properties of the system. It is shown that the two models give rise to almost the same behavior. The qualitative and quantitative characteristics of the two systems are the same. Both give rise to a maximum in the yield of ethanal as a function of heat transfer coefficient. They both predict the Hopf bifurcations accurately. The region of the dynamically unstable states occurs to the left of the point where the yield is a maximum in both models. They also show similar complex behavior in the repeated fed-batch mode of operation. We conclude that the behavior exhibited is not very sensitive to details in the model structure. It is also seen that the dynamic behaviors predicted by both the models are characterized by the same period-adding route. Thus, a detailed model where the variation of physical properties, *etc.*, is considered does not yield any new features. The route to complex periodic solutions can be captured by a simple model as can be seen by comparing Tables 3 and 4.

Acknowledgements

The authors thank the German Bundesministerium für Bildung und Forschung for financial support.

Appendix

The heat transfer from the reaction mixture to the coolant coil in the detailed model is calculated by [see eqn. (18)]:

$$(UA)_{cool}(T - T_{cool, in}) \tag{23}$$

where T signifies the reactor temperature, $T_{cool, in}$ is the inlet temperature of the coolant water and $(UA)_{cool}$ is the overall heat transfer coefficient. The overall resistance of the heat transfer $1/(UA)_{cool}$ is composed of the four resistances R_a, R_b, R_c and R_d:[27]

$$(UA)_{cool} = \frac{1}{R_a + R_b + R_c + R_d} \tag{24}$$

R_a describes the convective and diffusive heat transfer from the bulk of the reactor contents to the outer surface of the cooling coil. R_b specifies the resistance due to the thermal conductivity of the steel of the cooling coil. R_c signifies the heat transfer resistance between the inner surface of the cooling coil and the bulk of the coolant water. Finally, R_d describes the heat removal by the coolant. The resistances depend on the geometry of the cooling coil, the thermal conductivities of the reaction mixture, the coolant and the material of the cooling coil, for example. R_d is of special interest for our investigations with the detailed model because it is a function of the coolant flow $\dot{q}_{cool}$ which is used as a bifurcation parameter in this model:

$$R_d = \frac{1}{\dot{q}_{cool}\,\rho_{cool}\,c_{p,\,cool}\left[1 - \exp\left(-\dfrac{\alpha_{cool}\,A_w}{\dot{q}_{cool}\,\rho_{cool}\,c_{p,\,cool}}\right)\right]} \tag{25}$$

ρ_{cool} and $c_{p,\,cool}$ are the density and the specific heat capacity of the coolant water. These quantities are calculated by correlations given in ref. 20. In eqn. (25) α_{cool} denotes the heat transfer coefficient at the coolant side of the coil and A_w is the
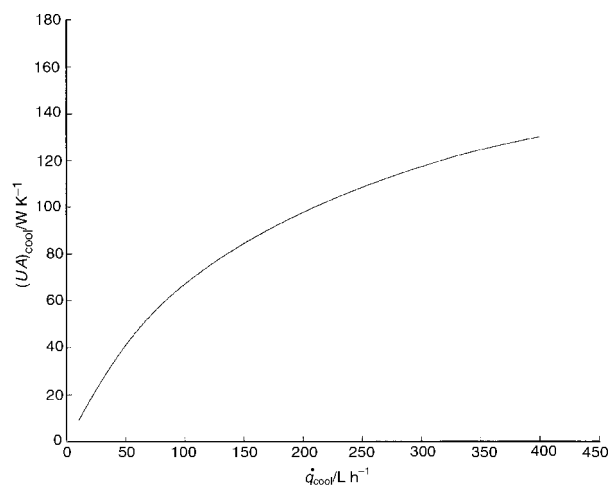

Fig. 8 The relation between the heat transfer coefficient $(UA)_{cool}$ (bifurcation parameter in the simple model) and the coolant flow rate $\dot{q}_{cool}$ (bifurcation parameter in the detailed model) is depicted for the parameter set given in the caption of Fig. 2a.

surface of the cooling coil. In Fig. 8 the relation between the heat transfer coefficient $(UA)_{cool}$ and the volumetric coolant flow rate $\dot{q}_{cool}$, which are used as bifurcation parameters in the simple and in the detailed model, respectively, is shown.

References

1 C. van Heerden, *Chem. Eng. Sci.*, 1958, **8**, 133.
2 R. Aris and N. R. Amundson, *Chem. Eng. Sci.*, 1958, **7**, 121.
3 E. D. Gilles and H. Hofmann, *Chem. Eng. Sci.*, 1961, **15**, 328.
4 A. Uppal, W. H. Ray and A. B. Poore, *Chem. Eng. Sci.*, 1974, **29**, 967.
5 V. S. Sheplev, S. A. Treskov and E. P. Volokitin, *Chem. Eng. Sci.*, 1998, **53**, 3719.
6 D. V. Jorgensen and R. Aris, *Chem. Eng. Sci.*, 1983, **38**, 45.
7 J. C. Mankin and J. L. Hudson, *Chem. Eng. Sci.*, 1984, **39**, 1807.
8 J. M. Douglas and D. W. T. Rippin, *Chem. Eng. Sci.*, 1966, **21**, 305.
9 D. Sinčić and J. E. Bailey, *Chem. Eng. Sci.*, 1977, **32**, 281, and references therein.
10 A. Stankiewicz and M. Kuczynski, *Chem. Eng. Process.*, 1995, **34**, 367, and references therein.
11 J. Lazar and J. Ross, *Science*, 1990, **247**, 189.
12 W. Hohmann, D. Lebender, J. Müller, N. Schinor and F. W. Schneider, *J. Phys. Chem. A*, 1997, **101**, 9132, and references therein.
13 R. B. Codell and A. J. Engel, *AIChE J.*, 1971, **17**, 220.
14 J. Ausikaitis and A. J. Engel, *AIChE J.*, 1974, **20**, 256.
15 Z. Kubíčková, M. Kubíček and M. Marek, *Chem. Eng. Sci.*, 1987, **42**, 327.
16 R. Konnur and S. Pushpavanam, *Chem. Eng. Sci.*, 1994, **49**, 383.
17 C. Hafke and E. D. Gilles, *Messen, Steuern, Regeln*, 1968, **11**, 204.
18 C. Hafke, Dissertation, Universität Stuttgart, 1972.
19 B. N. Figgis and G. B. Robertson, *Nature*, 1965, **205**, 694.
20 T. E. Daubert and R. P. Danner, *Physical and Thermodynamic Properties of Pure Chemicals Data Compilation*, Hemisphere Publishing, New York, 1989.
21 Verein Deutscher Ingenieure, *VDI-Wärmeatlas, Berechnungsblätter für den Wärmeübergang*, VDI, GVC, Düsseldorf, 1994.
22 C. Majer, Dissertation, Universität Stuttgart, 1997.
23 M. A. Alós, T. Obertopp, M. Mangold and E. D. Gilles, *Praxis Sicherheitstech.*, 1997, **4**, 293.
24 K.-P. Zeyer, M. Mangold, T. Obertopp and E. D. Gilles, *J. Phys. Chem. A*, 1999, **103**, 5515.
25 K.-P. Zeyer, M. Mangold, T. Obertopp and E. D. Gilles, *Chem. Eng. Sci.*, 1999, **54**, 4845.
26 M. Mangold, A. Kienle, E. D. Gilles and K. D. Mohl, *Chem. Eng. Sci.*, 2000, **55**, 441.
27 T. Obertopp, M. A. Alós, M. Mangold and E. D. Gilles, *Automatisierungstechnik*, 1999, **47**, 501.
28 J. M. Mansfield, R. A. Pulley and J. A. Wilson, *IChemE Res. Event*, 1995, 484.